

A study on electromagnetic property during friction stir weld failure

S. Muthukumaran · Kumar Pallav ·
Vikas Kumar Pandey · S. K. Mukherjee

Received: 19 March 2006 / Accepted: 10 October 2006 / Published online: 12 December 2006
© Springer-Verlag London Limited 2006

Abstract Electromagnetic radiation is emitted during the transient stage of elastic to plastic deformation of metals and alloys. In the present work, aluminium plates were welded by friction stir welding (FSW) at different process parameters, such as tool rotational speed, traverse speed and rake angle. The EMR fundamental frequencies emitted during the tensile failure of the welds were measured and recorded. The variation in the fundamental frequency was analysed by fuzzy modelling using MATLAB and it was observed that an increase in the first mode of metal transfer decreases the fundamental frequency. Further, the fundamental frequency of a weld was estimated from the obtained model and found to be closer to the experimental results. This work will be more useful for metal flow analysis as well as online condition monitoring of the welds which are used in critical applications.

Keywords Friction stir welding · Electromagnetic radiation · Welding parameters · Fuzzy modelling

1 Introduction

A stress-induced electromagnetic radiation (EMR) occurs during the transient stage of elastic to plastic deformation of metals and alloys under tension, compression, torsion and impact traction [1–5]. Friction stir welding (FSW) is a new solid state welding process in which a rotating cylindrical tool with a pin at the bottom is plunged into a rigidly held workpiece and traversed along the joint to be welded as shown in Fig. 1. FSW has several advantages over the fusion welding processes such as higher joint strength and the elimination of various solidification defects. A wide variety of both similar and dissimilar aluminium alloys have been successfully welded by this technique. Substantial development in FSW has been achieved in last decade in areas such as flow analysis, modelling and the study of metallurgical and mechanical properties [6–8]. However, this is the first work reporting the variation of EMR properties during the tensile failure of FSW welds.

2 Instrumentation for EMR study

It has been well established that the EMR emission is uninfluenced by stray external fields, but the latter do affect the instrumentation [3–5]. Therefore, experiments were conducted in the electro-statically shielded chamber of the laboratory. A horizontal Hounsfield tensometer (1.0 tonne capacity; Hounsfield Test Equipment, UK) was used for loading the specimen. The tensometer was operated at the best possible uniform speed of loading.

Experimental and theoretical research of the past [1–5] has shown the following possible mechanisms of EMR

S. Muthukumaran (✉) · S. K. Mukherjee
Department of Production Engineering,
Birla Institute of Technology,
Mesra, Ranchi 835215, India
e-mail: mrsrmuthu@hotmail.com

K. Pallav · V. K. Pandey
Department of Mechanical Engineering,
Birla Institute of Technology,
Mesra, Ranchi 835215, India

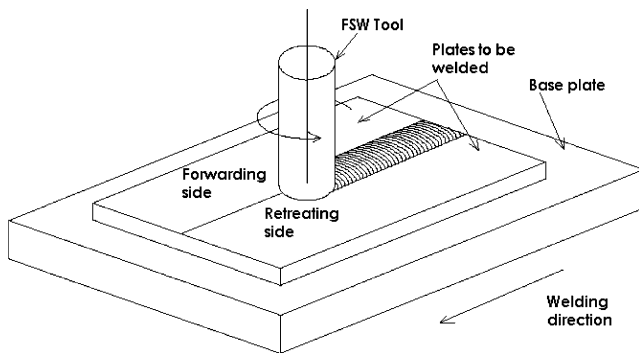


Fig. 1 The friction stir welding process

generation: (i) dislocation–dislocation interaction giving rise to EMR emission in KHz frequency range, (ii) dislocation–electron interaction giving rise to EMR emission in MHz frequency range, and (iii) electron–electron interaction giving rise to EMR emission in the GHz frequency range. The EMR signal of our interest in FSW failure is dislocation–dislocation interaction. Hence, for the detection of the EMR signals, an inverted U-shaped antenna, made of 0.34 mm copper sheet (18 mm height, 12 mm wide, U-bottom diameter 5 mm) was used for the study (Fig. 2).

An analog-digital HAMEG oscilloscope (HM 1,507–3; Hameg Instruments, Mainhausen, Germany) and one 199 Fluke ScopeMeter (Fluke Corp., Everett, WA, USA) incorporating the SCC190 accessory kit (RS 232 adapter and Fluke software) were used to record the signals. The software built within the HAMEG oscilloscope had fast Fourier transform (FFT) facility to convert time domain EMR signals into frequency domain. A Pentium IV personal computer was used for data storage and processing. Further, one lead of a 1 MW impedance cable was connected to the antenna and the other lead was connected to the Hounsfield tensometer to which the specimen were mounted for loading. Furthermore, the trigger level of the oscilloscope was kept just above the noise level of the laboratory to avoid the interference of noise with the signal.

In the present study many aluminium plates were welded by the FSW process and EMR specimen were prepared. The EMR radiation was captured during tensile failure of the specimen and the results obtained were analysed by a fuzzy modelling. Furthermore, the fundamental frequency was estimated from the model for the



Fig. 2 Photograph of antenna used in the experiment

Table 1 Process parameters adopted for FSW in the present study

Parameter	Value/Description		
Tool rotational speed (rpm)	900	1120	1400
Traverse speed (mm/min)	125	160	200
Rake angle (°)	0	1	2
Type of edge preparation	Manual	Wire cut EDM	–

unknown process parameters and compared with the experimental results.

3 Experimental work

A modified 2369-0 HMT universal milling machine was used for friction stir welding of 6.3 mm Al 6063-T4 aluminium plates of composition Al–Si0.4–Fe0.35–Cu0.1–Mn0.1–Mg0.7–Cr0.1–Zn0.1–Ti0.1. Two FSW tools were made of tool steel with shoulder diameters of 13 and 15 mm and the process parameter ranges adopted in the present study are shown in Table 1 below.

A Taguchi L_{18} orthogonal array [9] was selected in order to minimize the number of experiments required on the various combinations of the process parameters. The edges of the aluminium plates were prepared and clamped firmly to a base plate. Welding was performed under different sets of parameters corresponding to the L_{18} orthogonal array. The specimen for EMR study were prepared from each of the welded plates with a notch at the centre. The notches were prepared by electron discharge machining (EDM) and the specimen dimensions adopted are shown in Fig. 3.

The experimental arrangement for the EMR study is shown in Fig. 4. When tensile force was gradually applied to the specimen, the transient stage of elastic to plastic deformations occurred in the weld zone resulting in EMR emission. Due to further loading the specimen was fractured along the notch and a fractured specimen is shown in Fig. 5. The antenna was connected to the oscilloscope through probes and the signals were saved in the computer. Further, these signals were analysed by the FFT analysis using HAMEG software to determine the fundamental frequency.

4 Results and discussion

An EMR signal captured during tensile fracturing of a specimen and the corresponding result obtained by FFT analysis are shown in Figs. 6 and 7, respectively.

The different welding parameters adopted and the corresponding fundamental frequencies are shown in Table 2.

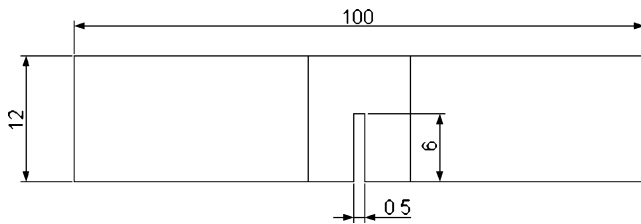


Fig. 3 Dimension (in mm) of the EMR specimen prepared from the FSW weld

A fuzzy modelling was done using MATLAB [10] to exhibit the variation in fundamental frequency with change in welding parameters. The results obtained by the fuzzy modelling are shown in Figs. 8, 9, 10, 11, 12. In most of the cases, it can be observed from the experimental results that there exists a critical relationship between the variation in welding parameters and the fundamental frequencies. Muthukumaran and Mukherjee [8] reported that two modes of metal flow occur during the FSW process. The first mode of metal transfer occurs layer by layer and is caused by tool shoulder, whereas the second mode of metal transfer is caused by extrusion around the pin. The increase in tool rotation speed or decrease in traverse speed brings about an increase in metal transfer by the first mode [8]. However, in many cases it is difficult to distinguish between the two modes in the weld macrostructures.

The increase in tool rotational speed from 900 to 1,400 rpm causes a decrease in the fundamental frequency by 0.07 KHz as shown in Fig. 8. Similarly, with an increase in traverse speed from 125 to 200 mm/min, the fundamental

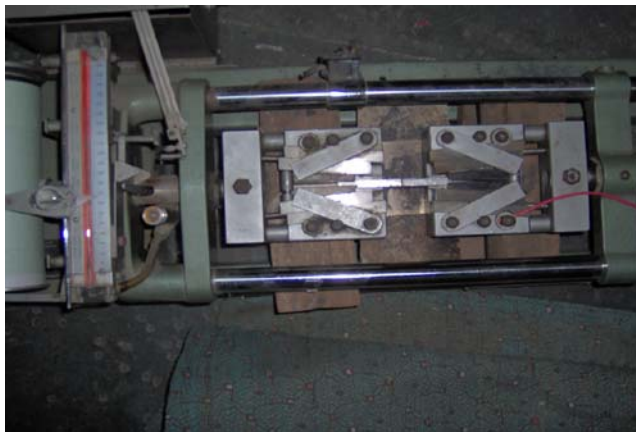


Fig. 4 Experimental arrangement for the EMR study showing a specimen in the Hounsfield tensometer



Fig. 5 Photograph of an EMR specimen after fracture

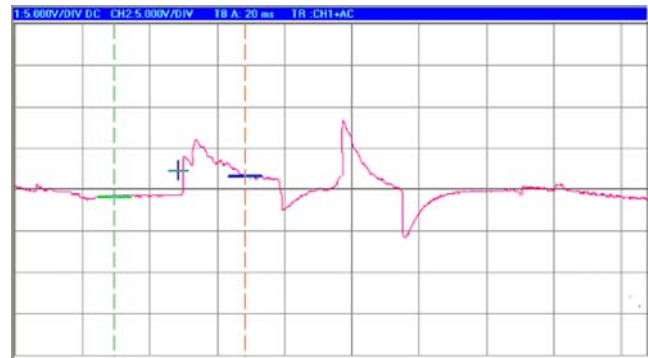


Fig. 6 Signal received during fracture of an EMR specimen

frequency was found to increase by 0.1 KHz as shown in Figs. 9 and 10. Hence, it is evident from these results that with an increase in first mode, the fundamental frequency of EMR signals decreases. Zhang et al. [11] showed that as the translational velocity increases, the maximum longitudinal residual stress also increases. This may affect the first mode of metal transfer and the fundamental frequency.

Furthermore, as the shoulder diameter increases from 13 to 15 mm, the fundamental frequency was found to decrease by 0.1 KHz at lower rake angles (LRA) as shown in Fig. 11. This shows that the first mode of metal transfer increases with an increase in the shoulder diameter. As the shoulder accelerates the material flow in the radial direction [12], an increase in shoulder diameter may increase the first mode of metal transfer. Similarly, as the rake angle increases from 0 to 2°, the fundamental frequency was found to increase by 0.3 KHz as shown in Figs. 8, 10 and 12. This shows that the first mode of metal transfer decreases with an increase in rake angle. Furthermore, the fundamental frequency was found to be higher for the weld made by manual edge preparation (0.6 KHz) than the weld made by wire cut EDM (0.35 KHz) as shown in Figs. 9 and 12. Hence, the first mode of metal transfer increases if the plates are in better match.

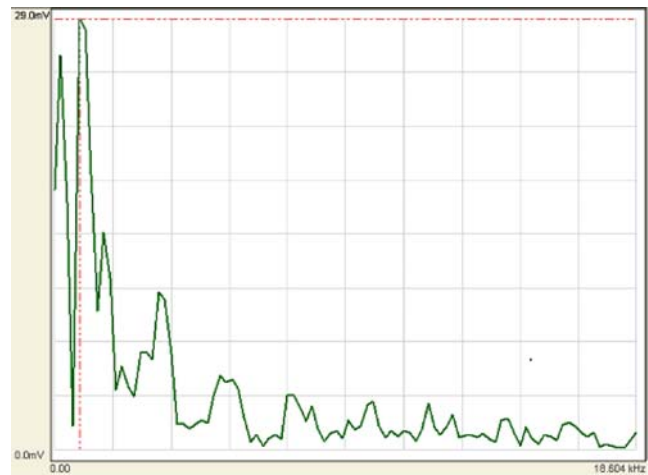


Fig. 7 Result obtained by FFT analysis by processing the EMR signal

Table 2 L_{18} orthogonal array depicting 18 different combinations of welding parameters along with the EMR frequencies during fracture

Specimen no.	Tool diameter (mm)	Tool rotation speed(rpm)	Traverse speed (mm/min)	Rake angle	Edge preparation	Fundamental frequency (KHz)
1	13	900	125	0	Manual	1.01
2	13	900	160	1	Manual	1.02
3	13	900	200	2	Wire cut EDM	0.6
4	13	1120	125	1	Wire cut EDM	0.797
5	13	1120	160	2	Manual	0.598
6	13	1120	200	0	Manual	0.752
7	13	1400	125	2	Wire cut EDM	0.589
8	13	1400	160	0	Manual	0.575
9	13	1400	200	1	Manual	0.612
10	15	900	125	1	Manual	0.589
11	15	900	160	2	Manual	1.18
12	15	900	200	0	Wire cut EDM	0.184
13	15	1120	125	0	Manual	0.398
14	15	1120	160	1	Wire cut EDM	0.401
15	15	1120	200	2	Manual	0.797
16	15	1400	125	2	Manual	0.672
17	15	1400	160	0	Wire cut EDM	0.376
18	15	1400	200	1	Manual	0.484

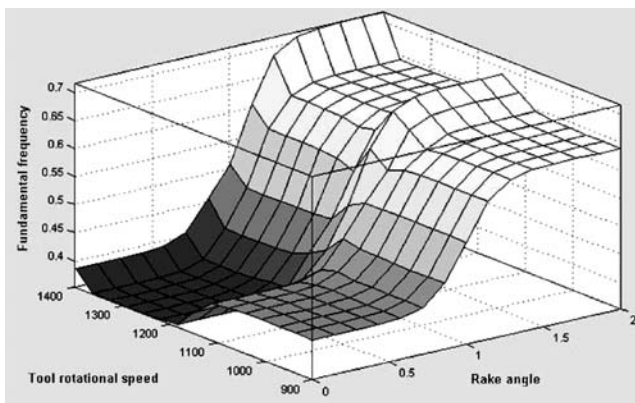
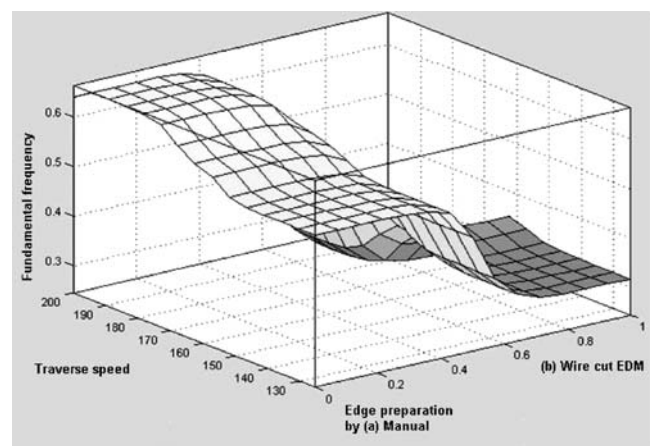
Thus, from the obtained fuzzy modelling it is possible to predict the fundamental frequency for any specimen welded under any set of process parameters within the chosen range. In order to measure precision of the result obtained by the fuzzy modelling, 6.3 mm plates were welded with the following process parameters:

Tool diameter	14 mm
Tool rotational speed	1,120 rpm
Rake angle	1.5°
Traverse speed	160 mm/min
Type of edge preparation	Manual

The measured fundamental frequencies for the two specimen were 0.78 and 0.77 KHz whereas the predicted fundamental frequency was 0.75 KHz. It can be observed that the error is less than 5% indicating closeness between the calculated and measured values.

5 Conclusion

In the present work, FSW was performed with different process parameters, EMR specimen were prepared and signals were captured during tensile failure. The obtained results were analysed by fuzzy modelling and the results

**Fig. 8** Effect of tool rotational speed and rake angle on fundamental frequency**Fig. 9** Effect of traverse speed and edge preparation on fundamental frequency

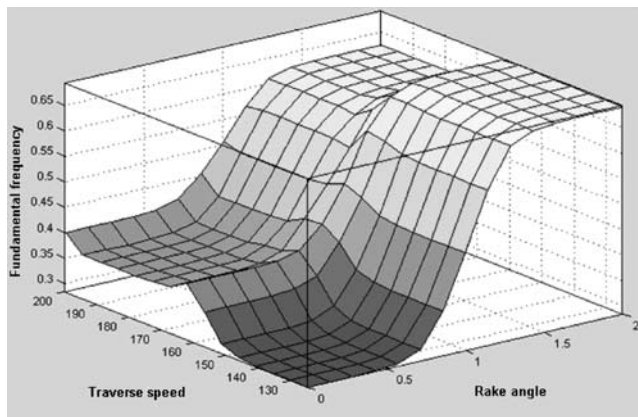


Fig. 10 Effect of traverse speed and rake angle on fundamental frequency

show that the decrease in the first mode of metal transfer increases the fundamental frequency. The result also shows that an increase in shoulder diameter from 13 mm to 15 mm and tool rotational speed from 900 to 1,120 rpm decreases the fundamental frequency by 0.1 and 0.07 KHz, respectively at LRA. However, with an increase in the traverse speed at LRA and the rake angle from 125 to 200 mm/min and 0 to 2°, the fundamental frequency was found to increase 0.1 and 0.3 KHz, respectively. This shows that the first mode increases with an increase in tool diameter and rotational speed at LRA and decreases with an increase in traverse speed and rake angle. Moreover, the first mode of metal transfer increases if the edges of the plates before welding are in better match. Furthermore, the fuzzy modelling is also useful for finding fundamental frequencies of any weld made within the chosen range. However, further study is necessary to understand the principle behind the decrease in the fundamental frequency with the first mode of metal transfer. In addition to the flow analysis, the present work is also more useful for online condition monitoring of the critical components made by the FSW process.

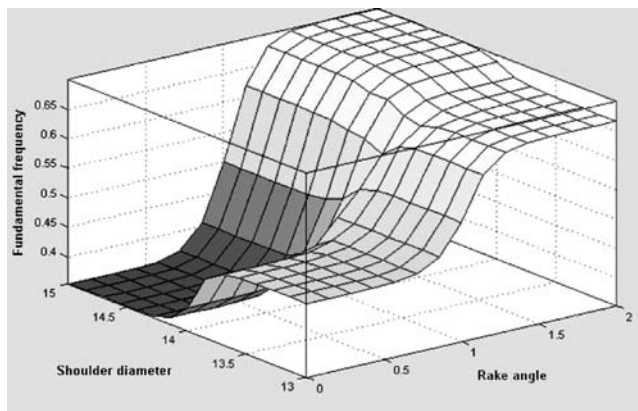


Fig. 11 Effect of shoulder diameter and rake angle on fundamental frequency

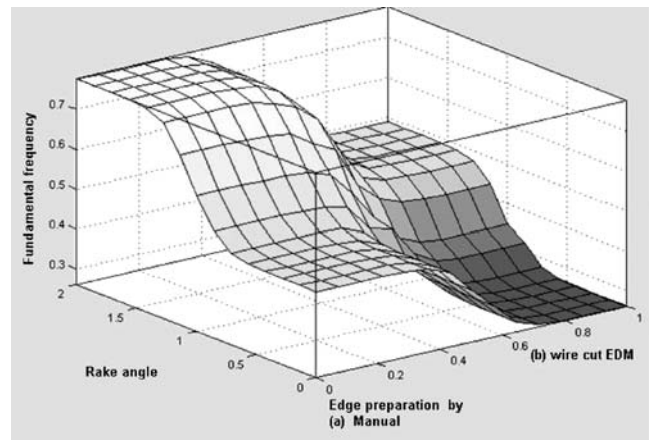


Fig. 12 Effect of rake angle and edge preparation on fundamental frequency

Acknowledgements The authors acknowledge Dr. Ashok Misra and Mrs. B. Srilakshmi for their kind co-operation in execution of the electromagnetic study and for their valuable suggestions to carry out this work. The valuable comments of the anonymous reviewers in improving the manuscript are thankfully acknowledged.

References

- Misra A (1975) Electromagnetic effects at metallic fracture. *Nature* 254:133–134
- Misra A (1978) A physical model for the stress induced electromagnetic effects in metals. *Appl Phys* 16:195–199
- Misra A (1981) Stress induced magnetic and electromagnetic effects in metals. *J Sci Indust Res* 40:22–23
- Srilakshmi B, Misra A (2005) Secondary electromagnetic radiation during plastic deformation and crack propagation in uncoated and tin-coated plain-carbon steel. *J Material Science* 40(23):6079–6086
- Misra A, Kumar A (2004) Some basic aspects of crack propagation in metals. *Int J Fract* 127:387–401
- Thomas WM, Needham ED, Murch ED, Templesmith P, Dawes CJ (1991) International patent application no. PCT/GB92/02203 and GB patent application no. 9125978.9
- Sahin AZ, Yilbas BS, Al-Garni AZ (1996) Friction welding of Al-Al, Al-steel and steel-steel samples. *J Mater Eng Perform* 5(1):89–99
- Muthukumaran S, Mukherjee SK (2006) Two modes of metal flow phenomenon in friction stir welding process. *Sci Technol Weld Joi* 11(3):337–340
- Park SH (1996) Robust design and analysis for quality engineering, 1st edn. Chapman & Hall, New York
- The MathWorks (2004) Fuzzy logic for use with MATLAB 6.1. The MathWorks Inc., Natick, MA, USA
- Zhang HW, Zhang Z, Chen JT (2005) The finite element simulation of the friction stir welding process. *Mater Sci Eng A* 403:340–348
- Zhang Z, Chen J, Zhang H (2005) The 3D simulation of friction stir welding process. Proceedings of ICMEM 2005 international conference on mechanical engineering and mechanics, 26–28 October, Nanjing, China, pp 1338–1342